ELSEVIER

Biochimica et Biophysica Acta 1565 (2002) 29–35

BIOCHIMICA ET BIOPHYSICA ACTA
BBA

www.bba-direct.com

Brownian dynamics simulation of the unsaturated lipidic molecules oleic and docosahexaenoic acid confined in a cellular membrane

Miguel X. Fernandes [a], Miguel A.R.B. Castanho [b,c], José García de la Torre [a,*]

[a] *Departamento de Química-Física, Facultad de Química, Universidad de Murcia, Campus de Espinardo, 30071 Murcia, Spain*
[b] *Centro de Química-Física Molecular, Instituto Superior Técnico, Av. Rovisco Pais, 1049-001 Lisbon, Portugal*
[c] *Departamento de Química e Bioquímica, Faculdade de Ciências da Universidade de Lisboa, Campo Grande, Ed. C8-6° Piso, 1749-016 Lisbon, Portugal*

Received 27 February 2002; received in revised form 24 May 2002; accepted 26 June 2002

Abstract

A Brownian dynamics (BD) simulation of two unsaturated molecules, oleic and docosahexaenoic acid, in an environment that reproduces a cellular membrane, is presented. The results of the simulations, performed using mean-field potentials, were calibrated with experimental results obtained for oleic acid in a cellular membrane. The agreement between simulation and experimental results is excellent which validates subsequent simulation outcome for docosahexaenoic acid. This molecule is a major component of several cellular membranes thought to be involved in specific biological functions that require conformational changes of membrane components. The results for docosahexaenoic acid indicate that it is minimally influenced by temperature changes and that it presents great conformational variability.

Keywords: Unsaturated lipid; Computer simulation; Brownian dynamics

1. Introduction

Biological membranes are highly organized ensembles of several different types of molecules whose structures and functions are interwoven. Restricting the focus on their lipidic matrix, we would still have hundreds of molecules. Among these, the polyunsaturated lipids are thought to increase and maybe regulate the fluidity state of the membranes [1]. However, it is not very consensual how unsaturated phospholipids play their role in biological membranes and, in fact, there are some prevailing contradictions when correlation between unsaturation degree of phospholipids and the fluidity state of membranes is made. Unsaturation lowers the phase transition temperature of phospholipids allowing biological membranes to maintain their fluid state at physiological temperature [1]. Besides this general physical feature, unsaturated lipids are implicated in specific biochemical functions in membranes of neurons [2], retinal rod cells [3] and spermatozoa [4], and therefore, the study of equilibrium and dynamical properties of unsaturated molecules is of general interest and relevance.

Docosahexaenoic acid, DHA, is a polyunsaturated fatty acid that has been the subject of several nutritional, biological and physiological studies (e.g. Refs. [5–7]). On the other hand, scarce studies deal with the physical and chemical properties of DHA as a biological membrane constituent. The latter type of studies includes the influence on the conformation of phosphatidylcholines [8], interaction with cholesterol in vesicles [9], NMR studies of multilamellar dispersions [10] and modeling by conformational space search [11,12]. Concerning the action of DHA, spectroscopic studies suggest that this molecule has an increased lateral compressibility and conformational freedom relatively to saturated phospholipids acyl chains and that adapts faster to configuration changes of neighboring molecules [13–15]. Modeling studies of DHA produced divergent conclusions: in one of them, a rigid and ordered character was established for the molecule [11], while in the other attributes, maximum conformational freedom and low sensitiveness to temperature effects was concluded [12].

The experimental studies of molecules in membranes are very difficult and detailed atomic level properties hard to get.

* Corresponding author. Tel.: +34-96-8367426; fax: +34-96-8364148.
E-mail address: jgt@um.es (J. García de la Torre).
URL: http://leonardo.fcu.um.es/macromol/.

0005-2736/02/$ - see front matter
PII: S0005-2736(02)00501-1

Fluorescence spectroscopy and NMR studies of unsaturated lipids in membranes provide information on both equilibrium and dynamical properties but to gain atomic level understanding of those properties of unsaturated molecules, we have used computer simulation. Probably, molecular dynamics (MD) is the most frequently used technique to simulate bilayer systems (for a review, see Ref. [16]). However, in spite of its more detailed description of a system, due to an all-atom representation, MD is limited to short time range simulations, generally within the order of picoseconds. We use Brownian dynamics (BD) to simulate a single molecule and, therefore, reach long time range simulations. The influence of other molecules that constitute the system, on the simulated one, is described by the mean-field potentials used in this approach. Previously, Langevin and BD simulation, which are stochastic techniques, were used to simulate a DPPC bilayer in the liquid-crystal [17,18] and gel [19] states and also unsaturated molecules in a bilayer environment [19,20].

The most suitable and useful system to be simulated would be a cellular membrane because DHA is a major component of some cellular membranes and thought to be involved in specific physiological events. A single molecule simulation with atomic level detail of an oleic acid molecule and of a DHA molecule was performed. We made the option for the reproduction of an oleic acid molecule properties in a biological membrane, having in mind that subsequently, we would extend our studies to the case of DHA. As oleic acid has a double bond in *cis* conformation and DHA has six double bonds with the same conformation, the previous simulation of oleic acid seems to be a natural choice. The experimental results here used to calibrate our mean-field potentials were obtained from an oleyl enriched biological membrane, which is very similar to the biological systems where DHA would be naturally present. Having reproduced correctly the features of an oleic acid molecule in a biological membrane with a high component of unsaturated acyl chains, we simulated the properties of a DHA molecule in the same membrane system.

2. Model and simulation procedures

2.1. Model

One of the systems that we simulate has 18 spherical elements joined by frictionless connectors and models the structure of an oleic acid molecule, which has a double bond between C atoms 9 and 10. This molecule is placed in a model membrane of finite thickness and none of the spheres, which represent methyl and methylene groups (one of the spheres represents the carboxylic group), can trespass the simulated membrane boundaries which means that the movement is confined in the z direction (see Fig. 1). The chain-model generally extends itself in one of the layers of the bilayer, meaning in the $[0, z_0]$ or $[-z_0, 0]$ domains.

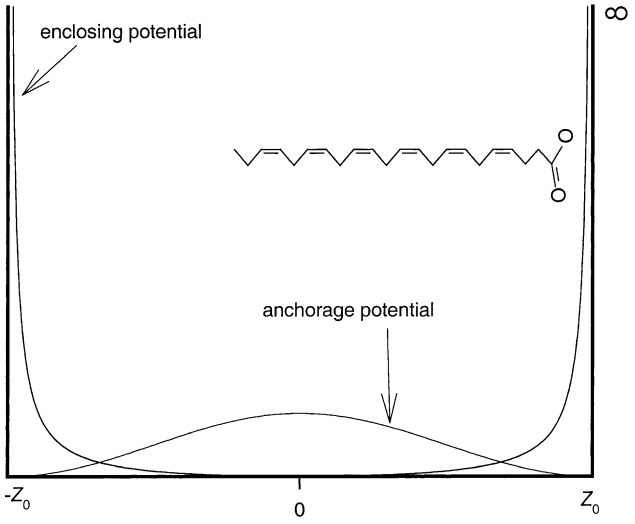

Fig. 1. Structure of docosahexaenoic acid and simulated system.

In the other system which represents the case of DHA, we used a 22-element chain that reproduces the structure of that fatty acid, which has six double bonds at positions 4, 7, 10, 13, 16, and 19 (see Fig. 1). The carboxyl group was substituted by a pseudo-atom that tends to be anchored at the membrane boundary. Once again, the movement of this molecule is confined in the z direction.

2.2. Intramolecular energetics

The internal energy of simulated molecules has contributions resulting from stretching, bending, torsional and non-bonded interaction energy. More clearly, the stretching potential, V_{stretch}, maintains the bond length between any two consecutive elements of a simulated molecule and it has a harmonic type expression in l (l is the distance between two consecutive elements)

$$V_{\text{stretch}}(l_i) = \frac{1}{2}K_{l,i}(l_i - l_{0i})^2 \quad (1)$$

where $K_{l,i}$ is the constant for the potential that joins elements i and $i+1$, l_i is the instantaneous distance between those two elements and l_{0i} is the equilibrium distance between the same elements. The angle between any three consecutive elements of simulated molecules is maintained by the bending potential, V_{bend}, that also has a harmonic type expression in α (α is the angle formed by three consecutive elements)

$$V_{\text{bend}}(\alpha_i) = \frac{1}{2}K_{\alpha,i}(\alpha_i - \alpha_{0i})^2 \quad (2)$$

where $K_{\alpha,i}$ is the constant for the potential that joins elements i, $i+1$ and $i+2$; α_i is the instantaneous bond angle between those three elements; and α_{0i} is the equilibrium angle between the same elements. The torsional potential, V_{torsion}, which is represented by a power series of cos ϕ (ϕ is the dihedral angle formed by four consecutive elements) was introduced by Ryckaert and Bellemans [21] in alkane chains

and accounts for the contribution of dihedral angles for the total internal energy of the simulated molecule.

$$V_{\text{torsion}}(\phi_i) = \sum_{k=0}^{5} c_k(\cos\phi_i)^k \quad (3)$$

where ϕ_i is the instantaneous values of the dihedral angle formed by elements i, $i+1$, $i+2$ and $i+3$ and c_k are constants. In the case of oleic acid and DHA, we have to perform slight modifications in the expression for the torsional potential due to the presence of double bonds. The torsional potential expression [22] for dihedral angles around sp^2–sp^3 C−C bonds is given by

$$V_{\text{torsion}}(\phi_i) = c_1(1+\cos\phi_i) + c_2(1+\cos(2\phi_i)) + c_3(1+\cos(3\phi_i)) \quad (4)$$

and the rotation around sp^2–sp^2 C−C bonds is restricted [22] using the expression

$$V_{\text{torsion}}(\phi_i) = K_{\text{torsion}}(\cos\phi_i - \cos\phi_{0i})^2 \quad (5)$$

where K_{torsion} is a constant, ϕ_i is the dihedral angle and ϕ_{0i} is 180° (all double bonds are in *cis* conformation). The non-bonded potential, V_{LJ}, represents the contributions due to van der Waals interactions between elements i and j ($j \geq i+4$). The expression of this potential has the following expression

$$V_{LJ} = 4\varepsilon\left(\left(\frac{\sigma}{r_{ij}}\right)^{12} - \left(\frac{\sigma}{r_{ij}}\right)^{6}\right) \quad (6)$$

The magnitudes [22,23] used for all the above described potentials are presented in Table 1.

Table 1
Intermolecular potentials values

Lennard–Jones potential	
Parameter	Value
σ	3.92 Å
ε	0.144 kcal mol^{-1}
Torsion potential	
Parameter	Value (kcal mol^{-1})
c_0	1.941
c_1	3.730
c_2	−1.071
c_3	−3.703
c_4	2.141
c_5	−3.034
Bending potential	
Parameter	Value
α_0	114°
K_α	124 kcal mol^{-1} rad^{-2}
Stretching potential	
Parameter	Value
b_0	1.53 Å
K_b	250 kcal mol^{-1} Å^{-2}

2.3. Mean-field potentials

The mean-field that simulates a bilayer environment has contributions resulting from:

(1) enclosing potential that emulates the finite thickness (along the z-axis) of the membrane and also the hydrophilic nature of membrane interfaces;

$$V_{\text{encl}}(z_i) = K_{\text{encl}}\frac{kT}{(z_0^2 - z_i^2)} \quad i = 2,\ldots,N \quad (7)$$

where K_{encl} is the potential constant, k is the Boltzmann constant, T is the absolute temperature, z_0 is the membrane interface coordinate, z_i is the coordinate of the i-th element and N is the number of elements.

(2) the anchorage potential that places elements which interact favorably with membrane interfaces in their vicinity;

$$V_{\text{anc}} = K_{\text{anc}}kT\cos^2\left(\frac{\pi z_1}{2z_0}\right) \quad (8)$$

where K_{anc} is the potential constant and z_1 is the coordinate of the element that represents the carboxylic group.

(3) the orientational potential that emulates the anisotropic medium of a bilayer and the ordering effect induced by acyl chains in neighboring molecules. The enclosing potential acts on all spheres but the one that represents the carboxylic group. Conversely, the anchorage potential only acts on the sphere that represents the carboxylic group. The expressions of these potentials were presented previously [18,24] and for the orientational potential, the expression is

$$V_{\text{orient}} = -\frac{3}{2}kTK_\theta(z)(\cos^2(\theta_i - \theta_{\text{tilt}}) - 1) \quad (9)$$

where θ_{tilt} is the tilt angle, θ_i is the angle formed by the segment that joins the atoms C_{i-1}−C_{i+1} and the bilayer normal, and $K_\theta(z)$ is the field strength of the orientational potential. $K_\theta(z)$ is not constant throughout the membrane, instead it changes linearly with z [18], reflecting the different packing of acyl chains in bilayers revealed by neutron diffraction studies [25], and θ_{tilt} is zero if the chain is parallel to the bilayer normal, which is the case of bilayers in the liquid-crystal state (θ_{tilt} can assume another value if a different orientation is expected).

2.4. Parameterization of mean-field

A systematic search for the mean-field potential magnitudes was carried out. Simulation results obtained for the oleic acid molecule, for each particular set of values of the mean-field potentials, were compared with experimental data for the same molecule and the set that gave the best fit was chosen to be used throughout the remaining work.

For instance, our search shows that: a higher value of the orientational potential will lead to a general raise in the order parameters, $-S_{CD}(i)$; a higher value of the anchorage potential will produce a small raise of $-S_{CD}(i)$ in the region near the interface; and a higher value of the enclosing potential has an effect of diminishing the $-S_{CD}(i)$ near the bilayer midplane. A more detailed description of the choice problem for the parameters magnitudes was presented elsewhere [18].

The anchorage potential field constant was set to 9.70×10^{-2} kJ mol^{-1}; the enclosing potential field constant has a value of 19.38 kJ Å^2 mol^{-1}; the orientational potential field constant employed was 6.2×10^{-2} kJ mol^{-1} at $z=z_0$ and 4.7×10^{-2} kJ mol^{-2} at $z=0$. With this choice of parameters, we recovered the experimentally determined order parameters [26] of an oleic acid molecule in a oleyl enriched cellular membrane at 314 K.

The simulations of the oleic acid molecule were performed for a bilayer half-thickness of 20 Å, at 314 K, a temperature for which this membrane is in the L_α phase. The simulations of DHA were performed in the same conditions presented above for the L_α phase, and also at 273 K. The system viscosity (which affects only the dynamics but not the conformational properties) was set to 0.025 P [17].

2.5. Dynamics algorithm

The trajectories of a single molecule, in each case, were simulated, with a computation time step of 4 fs and a total trajectory time of 200 ns, using a method based on the BD algorithm of Ermak-McCammon [27] with the predictor-corrector modification introduced by Iniesta and García de la Torre [28].

When simulating dynamic properties, we took into account the hydrodynamic interaction (HI) between elements of our system. For this purpose, we used the modified Oseen tensor [29,30] which corrects the effects of a non-point-like nature of friction elements and eventual overlapping. When simulating equilibrium properties, HI was neglected because equilibrium magnitudes do not depend on the rate of dynamic processes. BD without HI is considerably less computation time consuming than BD with HI.

3. Results and discussion

The results for the order parameter of the C–H segments which is given by

$$-S_{CD}^{i} = \left\langle \frac{3\cos^2\beta_i - 1}{2} \right\rangle \tag{10}$$

where β_i is the angle formed by the i-th C–H segment ant the membrane normal and the brackets denote an average over the entire trajectory. This parameter provides an indication of the orientational order of the oleic acid molecule (this parameter reflects both geometrical and motional effects) and from our simulation, it can be seen that this fatty acid presents higher values in the vicinity of the membrane interface (lower number carbon atoms) and that they drop as we move toward the membrane's midplane (higher number C atoms). There is a remarkable decrease in the order parameter of the atoms that are in contact with the atoms that form the double bond (this is an effect produced by double bonds on their neighboring atoms). The results obtained from simulation are in excellent agreement with the ones obtained experimentally [26] and the plot in Fig. 2 confirms this statement. The results for the order parameter profile of the DHA molecule are also plotted in Fig. 2. The DHA order parameters are considerably lower than the ones obtained for the oleic acid, specially in the region closer to the membrane interfaces. This points out toward: (1) a greater flexibility of the DHA and/or; (2) an orientation of the chain less parallel to the bilayer normal. At 41 °C, the DHA presents an almost flat order profile with few exceptions, namely atoms 5, 17, 18 and 19 while the others, though presenting some fluctuations, do not differ remarkably from an average value. We can also see in Fig. 2 that temperature has little effect on the behavior of DHA. The order parameters are almost invariant, with the change of temperature, exception made for the chain segment containing atoms 5–7. It should be stressed out that we assumed that temperature had no effect on the parameterization of the applied mean-field potentials (temperature is a variable in the motion equations but do not affect directly the magnitudes of the mean-field potentials). We did so because there is evidence that membranes containing DHA remain in a liquid-crystal-like phase at low temperatures [12]. If these membranes experienced a phase transition, we would have to change the parameterization of the mean-field [19].

The in-depth distributions, presented in Fig. 3 and in Table 2, of the C atoms of DHA show that they broaden on going from the carbonyl end toward the methyl end of the chain and that along the same direction, the distributions become slightly bimodal. One can see that the DHA chain

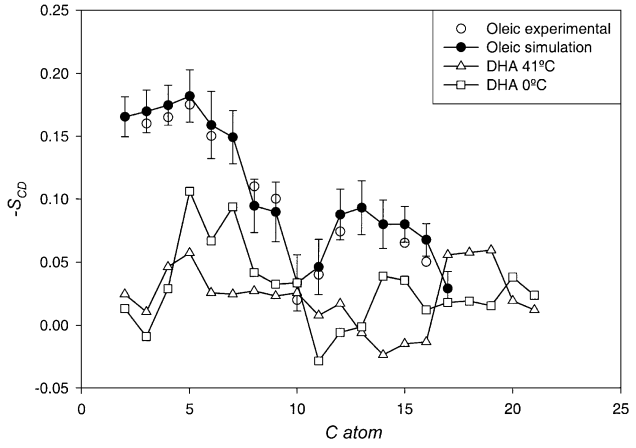

Fig. 2. Order parameters of C atoms of DHA and oleic acid.

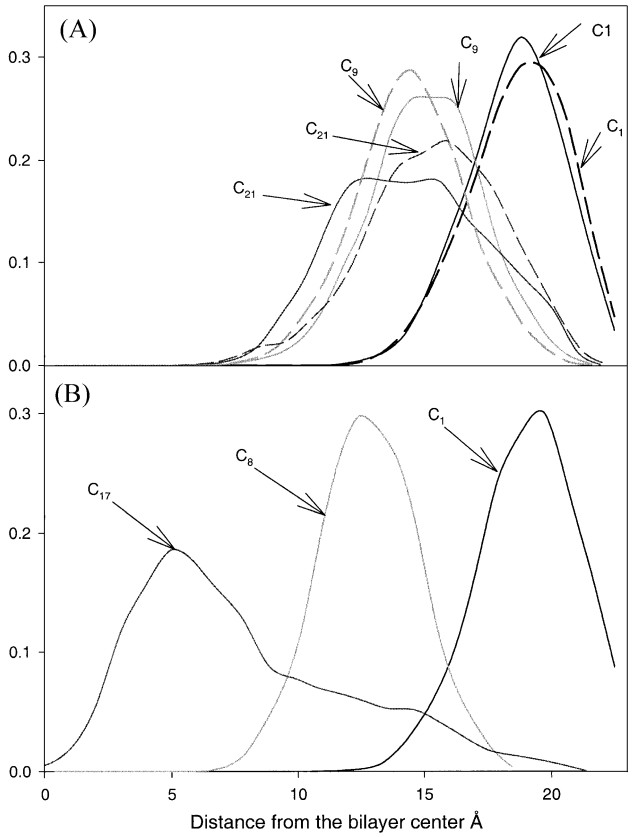

Fig. 3. In-depth distribution of C atoms: (A) DHA; (B) oleic acid. Dashed lines results at 0 °C and solid lines results at 41 °C.

occupies a narrower range of depths than the oleic acid molecule. All the DHA atoms are distributed between the interface and an imaginary plane placed at 6 Å from the membrane's midplane. The oleic acid atoms occupy a broad range of depths distributing themselves all over a membrane leaflet, presenting also a trend to broaden their distributions on going toward the methyl end of the chain. Comparing the mean of the distributions of each atom, we can see that DHA atoms occupy shallower positions than the equivalent atoms of the oleic acid molecule. Besides this feature, the C atoms distributions of oleic acid show a clearer trend of broadening as they are placed further away from the membrane's interface. Regarding the temperature effect on DHA, we can say that at 0 °C, the chain's methyl end is placed a little bit closer to the membrane's interface than at 41 °C. Besides this little difference, the similarities between the distribution of the C atoms for both temperatures are remarkable.

Table 2
Average in-depth position and standard deviation of carbon atoms

Carbon atom	Oleic acid		DHA 41 °C		DHA 0 °C	
	Average	Deviation	Average	Deviation	Average	Deviation
1	19.0	2.0	18.6	1.9	18.7	2.0
2	18.2	1.9	18.1	1.9	18.3	1.9
3	17.3	1.9	17.5	1.8	17.7	1.8
4	16.4	1.9	17.2	2.1	17.5	2.0
5	15.5	1.9	16.6	2.2	16.7	2.1
6	14.6	1.9	16.1	2.1	16.1	2.0
7	13.7	2.0	15.6	2.4	15.4	2.3
8	12.8	2.0	15.1	2.5	14.7	2.4
9	12.3	2.1	15.0	2.2	14.4	2.2
10	11.4	2.1	14.6	2.5	13.7	2.4
11	11.1	2.1	14.5	2.6	13.4	2.4
12	10.3	2.3	14.7	2.4	13.8	2.3
13	9.8	2.5	14.6	2.9	13.6	2.6
14	9.2	2.9	14.7	2.9	14.0	2.7
15	8.7	3.2	14.8	2.5	14.6	2.5
16	8.2	3.8	14.9	2.8	14.9	2.8
17	7.8	4.2	14.9	2.7	15.3	2.7
18	7.5	4.7	14.8	2.5	15.4	2.4
19	–	–	14.7	2.7	15.6	2.6
20	–	–	14.6	3.0	15.6	2.8
21	–	–	14.5	2.9	15.4	2.7
22	–	–	14.4	3.3	15.3	3.1

The results, at 41 °C, for the distribution of angles subtended between the DHA double bonds and the membrane normal, are presented in Fig. 4 and Table 3. It can be seen that, exception made for the first double bond, all double bonds present broader profiles than the one of oleic acid double bond. Furthermore, it is perceptible a trend to broaden the distribution of the angle, and also to become bimodal, as we move from the carboxyl end to the methyl end of the DHA molecule. The average of the distributions are also quite different when comparing the oleic acid

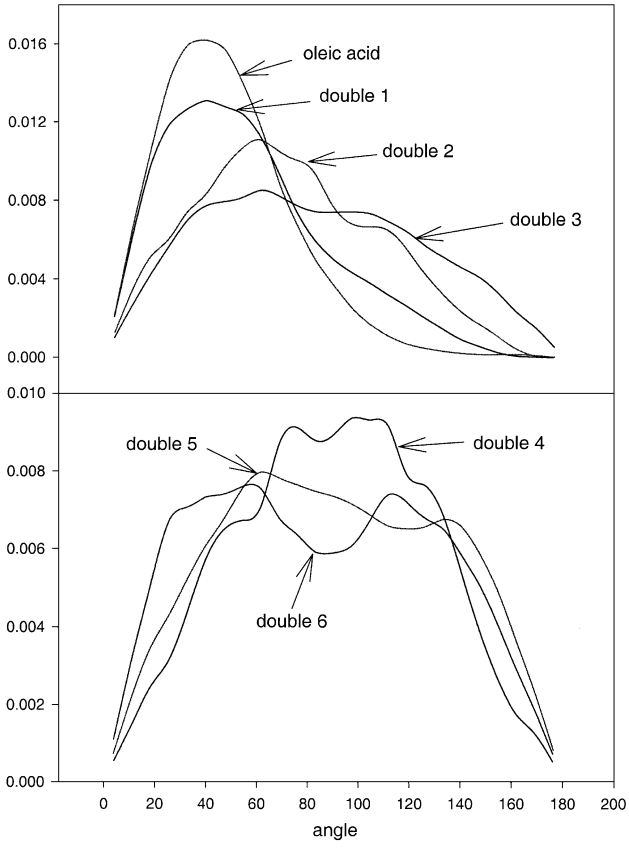

Fig. 4. Distribution of angle formed by double bonds and bilayer normal.

Table 3
Average angle (degrees) formed by double bonds and the bilayer normal and standard deviation

Double bond number	Oleic acid		DHA 41 °C		DHA 0 °C	
	Average	Deviation	Average	Deviation	Average	Deviation
1	48	26	56	32	51	29
2	–	–	65	35	51	29
3	–	–	82	41	75	35
4	–	–	92	36	108	37
5	–	–	90	42	109	37
6	–	–	82	44	89	42

molecule and DHA at 41 °C: the oleic acid molecule, that has its double bond at C9 presents an average value of 48° with a standard deviation of 26°, while for instance, DHA third double bond, located at C10, has an average value of 82° with a standard deviation of 41°. This indicates that this last double bond is generally almost perpendicular to the membrane normal and shows a great fluctuation around this average value. Comparing DHA at 41 and at 0 °C, we can see that at low temperature, DHA presents a lower angle value for the three first double bonds and higher values for the last three. This suggests that at 0 °C, the DHA chain is a little more stretched in the segment containing the three first double bonds (also confirmed by in-depth distribution results of these atoms in Table 2) and that there is a little more order (indicated by lower standard deviations) at this temperature.

The end-to-end distance of the oleic acid molecule has an average value of 14.2 Å with a standard deviation of 3.6 Å while DHA presents an average value of 8.2 Å at 41 °C (7.9 Å at 0 °C) and a standard deviation of 2.1 Å (1.9 at 0 °C), which could be considered short for a molecule with 22 C atoms. This is consistent with a DHA conformation with pronounced bends or twists of the chain to diminish the separation between both ends (a stretched chain would have a greater end-to-end distance), and that is what was found along the simulated trajectory and is depicted in Fig. 5. The conformation of Fig. 5 is the most frequent along the simulated trajectory, and it can be seen that DHA forms a right stranded helix though changing its parameters (length and diameter) with time. During the simulated trajectory, the end-to-end distance of the DHA molecule assumes values ranging from as low as 4.2 Å to as high as 17.0 Å which indicates great structural flexibility for this molecule.

The transition rates between conformations of dihedral angles for DHA and the oleic acid molecule are presented in Fig. 6. We considered that a transition occurred when the dihedral angle value overcame the potential barrier and crossed the corresponding dihedral angle potential local minimum. This way, temporary leaps are not counted as transitions. Assuming that the transitions are independent, the transition rate is obtained by division of the number of transitions by the total time spent in the original conformation. It can be seen that the transition rates from *trans* to *gauche* configuration of the oleic acid molecule are higher

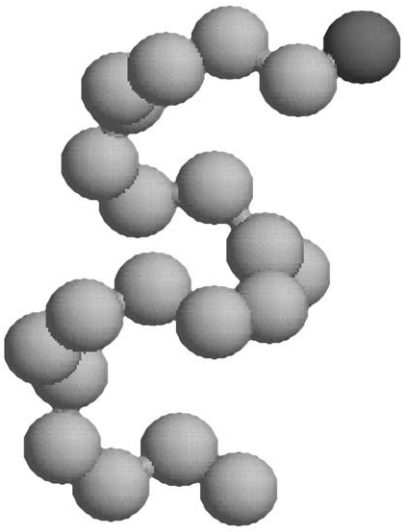

Fig. 5. Typical DHA helical structure found along the simulated trajectory. The dark sphere represents first carbon atom (carboxyl group).

at the extremities as it would be expected since terminal atoms have more rotational freedom than internal atoms. Furthermore, the transition rates for the dihedral angles that bracket the one that is centered in the double bond (dihedral 8) drop drastically when compared to neighboring dihedral angles. At 41 °C, the DHA molecule presents different results from the ones shown by oleic acid. Namely, only the first dihedral presents a noticeable transition, while the others have transition rates in the vicinity of 0. This means that all the double bonds restrain the rotational freedom of the internal atoms, even of those dihedral angles that do not present rotational restrictions.

The results here presented diverge from the ones presented by other computational studies [11,12] that postulated stretched conformations for the DHA molecules. Applegate and Glomset [11] postulated a rigid structure for the DHA molecule while Rabinovitch and Ripatti [12] postulated a flexible one, and our results indicate a flexible

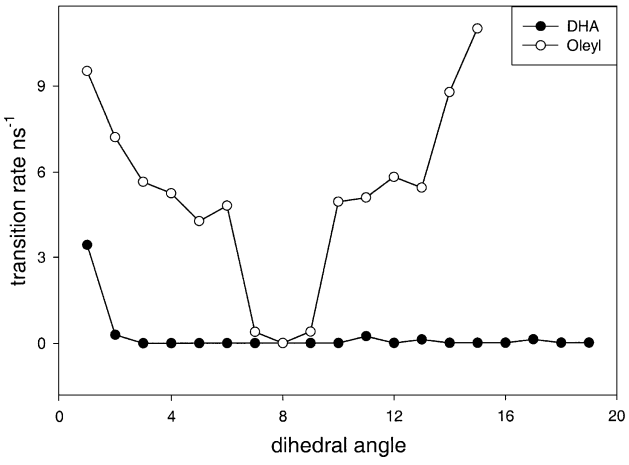

Fig. 6. Transition rate for dihedral angles of DHA and oleic acid.

structure though maintaining the same helical-type conformation found in those studies. The helix found in our studies is shorter and wider than the ones found before [11,12]. The difference between our results and the ones obtained previously derives from the dynamical character of our simulations compared to the static conformation space search of other studies [11,12]. Furthermore, the purpose of our work was to follow the dynamics of DHA in a cellular membrane environment, without any a priori restriction on the DHA structure. The objective of previous works [11,12] was to find a conformation that could allow optimal packing between DHA molecules. This is why we reached a helical conformation while previous works provided more stretched and symmetric conformations.

The insensitiveness of DHA to temperature is according to the proposed role of this molecule in biological systems which is the maintenance of conformational mobility of biomolecules in membranes under conditions of environmental temperature changes. Though the low-transition dihedral angle transition rates indicate local rigidities imposed by the double bonds, the helical conformation and the broad distributions for the angles formed by the double bonds and the membrane bilayer indicate that the DHA is flexible as a whole.

Acknowledgements

We thank Fundaç ão para a Ciência e Tecnologia (Portugal) for Grant SFRH/BPD/3594/2000 attributed to MXF and Grants PRAXIS/P/BIO/1279/1998 and POCTI/36458/QUI/2000 attributed to MARBC; Ministerio de Ciencia y Tecnologia (Spain) for Grant BQU2000-0229 attributed to JGT.

References

[1] P.R. Cullis, C.B. Hope, in: D.E. Vance, J.E. Vance (Eds.), Biochemistry of Lipids and Membranes, Benjamin Cummings Publishing, Menlo Park, CA, 1985.
[2] J.S. O'Brien, E.L. Sampson, J. Lipid Res. 6 (1965) 545–551.
[3] N.C. Nielsen, S. Fleischer, D.G. McConnell, Biochim. Biophys. Acta 211 (1970) 10–19.
[4] A. Darin-Bennet, A. Poulos, I.G. White, Andrologia 8 (1976) 37–45.
[5] M. Neuringer, W.E. Conner, C. Van Petten, L. Barstad, J. Clin. Invest. 73 (1984) 272–276.
[6] T. Farkas, K. Kitajka, E. Fodor, I. Csengeri, E. Lahdes, Y.K. Yeo, Z. Krasznai, J.E. Halver, Proc. Natl. Acad. Sci. U. S. A. 97 (2000) 6362–6366.
[7] C.A. Converse, H.M. Hammer, C.J. Packard, J. Sheperd, Trans. Ophthalmol. Soc. U. K. 103 (1983) 508–512.
[8] L. Holte, S.A. Peter, T.M. Sinnwell, K. Gawrisch, Biophys. J. 68 (1995) 2396–2403.
[9] D.C. Mitchell, B.J. Litman, Biophys. J. 75 (1998) 896–908.
[10] S. Everts, J.H. Davis, Biophys. J. 79 (2000) 885–897.
[11] K.R. Applegate, J.A. Glomset, J. Lipid Res. 27 (1986) 658–680.
[12] A.L. Rabinovich, P.O. Ripatti, Biochim. Biophys. Acta 1085 (1991) 53–62.
[13] B.W. Koenig, H.H. Strey, K. Gawrisch, Biophys. J. 73 (1997) 1954–1966.
[14] B.J. Litman, D.C. Mitchell, Lipids 31 (1996) S193–S197.
[15] T.S. Wiedmann, R.D. Pates, J.M. Beach, A. Salmon, M.F. Brown, Biochemistry 27 (1988) 6469–6474.
[16] D.P. Tieleman, S.J. Marrink, H.J.C. Berendsen, Biochim. Biophys. Acta 1331 (1997) 235–270.
[17] R.W. Pastor, R.W. Venable, M. Karplus, J. Chem. Phys. 89 (1988) 1112–1127.
[18] M.X. Fernandes, M.L. Huertas, M.A.R.B. Castanho, J. García de la Torre, Biochim. Biophys. Acta 1463 (2000) 131–141.
[19] M.X. Fernandes, J. García de la Torre, M.A.R.B. Castanho, J. Phys. Chem., B 104 (2000) 11579–11584.
[20] L.L. Pearce, S.C. Harvey, Biophys. J. 65 (1993) 1084–1092.
[21] J.P. Ryckaert, A. Bellemans, Chem. Phys. Lett. 30 (1975) 123–125.
[22] A. Rey, A. Kolinski, J. Skolnick, Y.K. Levine, J. Chem. Phys. 97 (1992) 1240–1249.
[23] G. Lamm, A. Szabo, J. Chem. Phys. 85 (1986) 7334–7348.
[24] M.L. Huertas, V. Cruz, J.J. López Cascales, A.U. Acuña, J. García de la Torre, Biophys. J. 71 (1996) 1428–1439.
[25] M.C. Wiener, S. White, Biophys. J. 61 (1992) 434–447.
[26] M. Rance, K.R. Jeffrey, A.P. Tulloch, K.W. Butler, I.C.P. Smith, Biochim. Biophys. Acta 600 (1980) 245–262.
[27] D.L. Ermak, J.A. McCammon, J. Chem. Phys. 69 (1990) 1352–1357.
[28] A. Iniesta, J. García de la Torre, J. Chem. Phys. 92 (1990) 2015–2019.
[29] J. Rotne, S. Prager, J. Chem. Phys. 50 (1969) 4831–4837.
[30] H. Yamakawa, J. Chem. Phys. 53 (1970) 436–443.